

Evidence for a Massive Dark Object in NGC 4350

Ezio Pignatelli[†], Paolo Salucci, and Luigi Danese

SISSA, via Beirut 4, I-34014 Trieste, Italy

17 November 2018

ABSTRACT

In this work we build a detailed dynamic model for a S0 galaxy possibly hosting a central massive dark object (MDO). We show that the photometric profiles and the kinematics along the major and minor axes, including the h_3 and h_4 profiles, imply the presence of a central MDO of mass $M_{\text{MDO}} \sim 1.5 - 9.7 \cdot 10^8 M_{\odot}$, i.e. 0.3 – 2.8% of the mass derived for the stellar spheroidal component. Models without MDO are unable to reproduce the kinematic properties of the inner stars and of the rapidly rotating nuclear gas.

The stellar population comprise of an exponential disc (27% of the light) and a diffuse spheroidal component (73% of the light) that cannot be represented by a simple de Vaucouleurs profile at any radius. The M/L ratios we found for the stellar components (respectively 3.3 and 6.6) are typical of those of disc and elliptical galaxies.

Key words: galaxies: individual: NGC 4350 – galaxies: kinematics and dynamics – galaxies: structure – galaxies: nuclei – dark matter

1 INTRODUCTION

There is increasing evidence that most galaxies with a large spheroidal component host a Massive Dark Object (MDO) at their centre, with masses ranging from $\sim 10^8 M_{\odot}$ to $2 \cdot 10^{10} M_{\odot}$ (Ho, 1999).

This evidence was first reviewed by Kormendy & Richstone (1995), suggesting that in kinematically hot galaxies (ellipticals and S0s) the mass of the central object M_{MDO} correlates with the mass of the hot stellar component M_{sph} . For the ratio $x \equiv \log(M_{\text{MDO}}/M_{\text{sph}})$ they found a Gaussian distribution with average value $x = -2.5$ and variance $\sigma = 0.2$. More recently, assuming isotropy in the velocity dispersion tensor, Magorrian et al. (1998) exploited the high resolution of HST photometry and ground based spectroscopy to estimate the MDO mass of 36 E/S0s, finding a similar correlation $x = -2.28 \pm 0.5$.

Exploiting the data from a sample of 30 galaxies, for which at least two independent MDO mass estimates are available, Salucci et al. (1999) found an average value $x = -2.60 \pm 0.3$, quite close to that obtained by Ho et al. (1999) and Ford et al. (1999). This result has been used to determine the mass function of MDOs hosted in spheroidal galaxies and turns out to be fully consistent with the mass function of accreted matter required to fuel QSO activity. This supports the idea that MDOs are the remnant BHs of a past era of nuclear galactic activity.

On the other hand, using several hundred rotation curves, Salucci et al. (2000) recently put stringent upper limits on the mass of the MDOs resident in late-type galaxies, showing that they must be on average at least 10–100 times smaller than the ones claimed for ellipticals. If one assumes that MDOs are the remnants of past QSO activity, this implies that the contribution to the shining phase of quasars by BHs hosted in late-type spirals is totally negligible.

Finally, recent results (Ferrarese & Merritt, 2000; Gebhardt et al., 2000a) showed that the central MDO mass strongly correlates with the galaxy velocity dispersion. In particular Gebhardt et al. (2000a) pointed out that ellipticals and bulges fall again in a fundamental plane when they are located in a four-dimension plane with coordinates $(M_{\text{BH}} - \log L - \log \sigma, \log R_e)$. This property implies some fundamental connection between the black hole and the bulge.

In this context it is interesting to investigate the role of S0 and early-type disc galaxies. In view of their massive bulge, they must be considered as a possible location for QSO remnants. However, the search for central massive objects in S0 is hampered, as: (1) the bulge/disc photometric decomposition is often uncertain; (2) these objects have weak $H\alpha$ lines and, consequently, the rotation curve inside the central 0.5 kpc cannot be accurately determined; (3) the rotation curve is too disturbed by the strong asymmetric drift effects to be representative of the circular velocity.

Detection of MDOs in this kind of galaxy requires kinematic data of the innermost regions, and a detailed dynamic model. This approach has proved effective in detecting mas-

[†] e-mail: pignat@si.ssa.it

Table 1. Properties of NGC 4350 (Tully, 1988). (1) Hubble type T ; (2) absolute blue magnitude B_T ; (3) total blue luminosity L_B ; (4) position angle P.A.; (5) observed apparent axial ratio at D_{25} ; (6) distance D ; (7) conversion scale from arcsec to parsec; (8) observed diameter at 25 mag/arcsec 2 isophote in blue.

(1) Type [T]	(2) B_T [mag]	(3) L_B [M_\odot]	(4) P.A. [$^\circ$]	(5) (b/a)	(6) D [Mpc]	(7) scale [pc/ $''$]	(8) D_{25} ['']
-2	11.94	$8 \cdot 10^9$	28	0.62	16.8	81.5	3.0

sive central dark objects in a few S0/Sa galaxies, including NGC 4594 (Kormendy *et al.*, 1996), M31 (Tsvetanov *et al.*, 1998), NGC 3115 (Emsellem *et al.*, 1999), and NGC 4342 (Cretton & Van Den Bosch, 1999). Given the highly compact stellar structure, central MDOs can only be detected through accurate reconstruction of the galactic components, including the bulge/disc decomposition.

The goal of this work is to investigate the possible presence of an MDO in the nucleus of the S0 galaxy NGC 4350, by applying the dynamical model of Pignatelli & Galletta (1999) to recent data. This work has been set out as follows: in Section 2 we present the available data; in Section 3 we give a brief summary of the hypothesis and characteristics of the model; in Section 4 we derive the best-fit parameters of the model; Section 5 is devoted to the discussion of the results and conclusions.

In this paper we assume a Hubble constant $H_0 = 75$ km s $^{-1}$ Mpc $^{-1}$.

2 THE DATA

NGC 4350 is classified as a classical S0 galaxy in the *Nearby galaxy catalog* (Tully 1988; see Table 1). It is observed almost edge-on (from its axial ratio one can infer an inclination angle $i > 62^\circ$).

For the photometry, we adopt the R-band surface brightness profiles published by Seifert and Scorz (1996). According to these authors, NGC 4350 can be decomposed into disc and bulge components. The disc is probably exponential, significantly decreasing beyond 40 arcsec; the bulge on the other hand dominates even in the outer parts of the galaxy, as indicated by the substantial drop in the ellipticity profile. No ring-like component, or inner stellar disc has been detected.

For the kinematics, we adopt Fisher's detailed stellar kinematical observations along the major and minor axis (Fisher, 1997). These include the rotational velocity, the velocity dispersion profile, and the profiles of the Gauss-Hermite higher-order moments h_3 , h_4 (Van Der Marel & Franx, 1993). Moreover, they also include emission-line gas kinematics of a rapidly rotating nuclear disc. The total number of independent measurements to be simultaneously fitted by a model is 280.

The high rotational velocity of the nuclear gaseous disc, the rapid increase of the stellar rotation curve in the first 2'' (≈ 160 pc) and the corresponding high peak in the velocity

dispersion profile suggest the presence of a central concentration of mass.

Loyer *et al.* (1998) modeled this galaxy in some detail using a Multi-Gaussian Expansion method. In this paper, the photometric and kinematic data are reproduced with a different method and the subsequent analysis is extended to include the gas rotational velocity and the profiles of the h_3 , h_4 parameters. As pointed out by several authors (Van Der Marel, 1999; Cretton & Van Den Bosch, 1999; Gebhardt *et al.*, 2000b), the use of the higher moments of the line-of-sight velocity distribution is very relevant in determining the orbital anisotropies, thus reducing the uncertainties on the MDO mass.

3 THE GALAXY MODEL

In order to investigate the gas and stellar kinematics we use the self-consistent dynamical technique of Pignatelli and Galletta (1999). We give here a brief summary of the technique and the general assumptions made.

A galaxy can be described by superposition of different components. For each component, we separately assume:

- the density distribution is oblate, without triaxial structures;
- the isodensity surfaces are similar concentric spheroids;
- the surface density profile follows a simple $r^{1/4}$ or an exponential law;
- the local velocity distribution is Gaussian;
- the velocity dispersion is isotropic ($\sigma_r = \sigma_\theta = \sigma_z$);
- the mass-luminosity ratio is constant with radius;

Our model does not consider the possible presence of triaxial structures (bar; triaxial bulge; tilted component; warp) or of anisotropy in the velocity distribution (with predominance of radial or tangential orbits).

The model has $4n + 2$ free parameters, where n is the number of adopted components: namely the luminosity, scale length, mass-luminosity ratio and flattening $\{L_{tot}, r_e, M/L, b/a\}$ of each component plus the inclination angle of the galaxy and the mass of the central massive dark object M_{MDO} . In principle, photometry can be used to constrain all these parameters except the M/L ratios and the value of M_{MDO} , which must be derived through the kinematics.

4 COMPARISON BETWEEN MODEL AND DATA

4.1 Photometry

Seifert and Scorz (1996) have performed detailed CCD photometry in the R-band for a sample of 16 early-type disc galaxies, including NGC 4350. For each galaxy, they determined the radial profiles for surface brightness and ellipticity, together with a bulge/disc decomposition without special assumptions on the radial density profiles of the two components. According to the authors, the disc of NGC 4350 extends up to the innermost regions of the galaxy and follows approximately an exponential law; the spherical component dominates both in the nucleus and in the outer parts, as

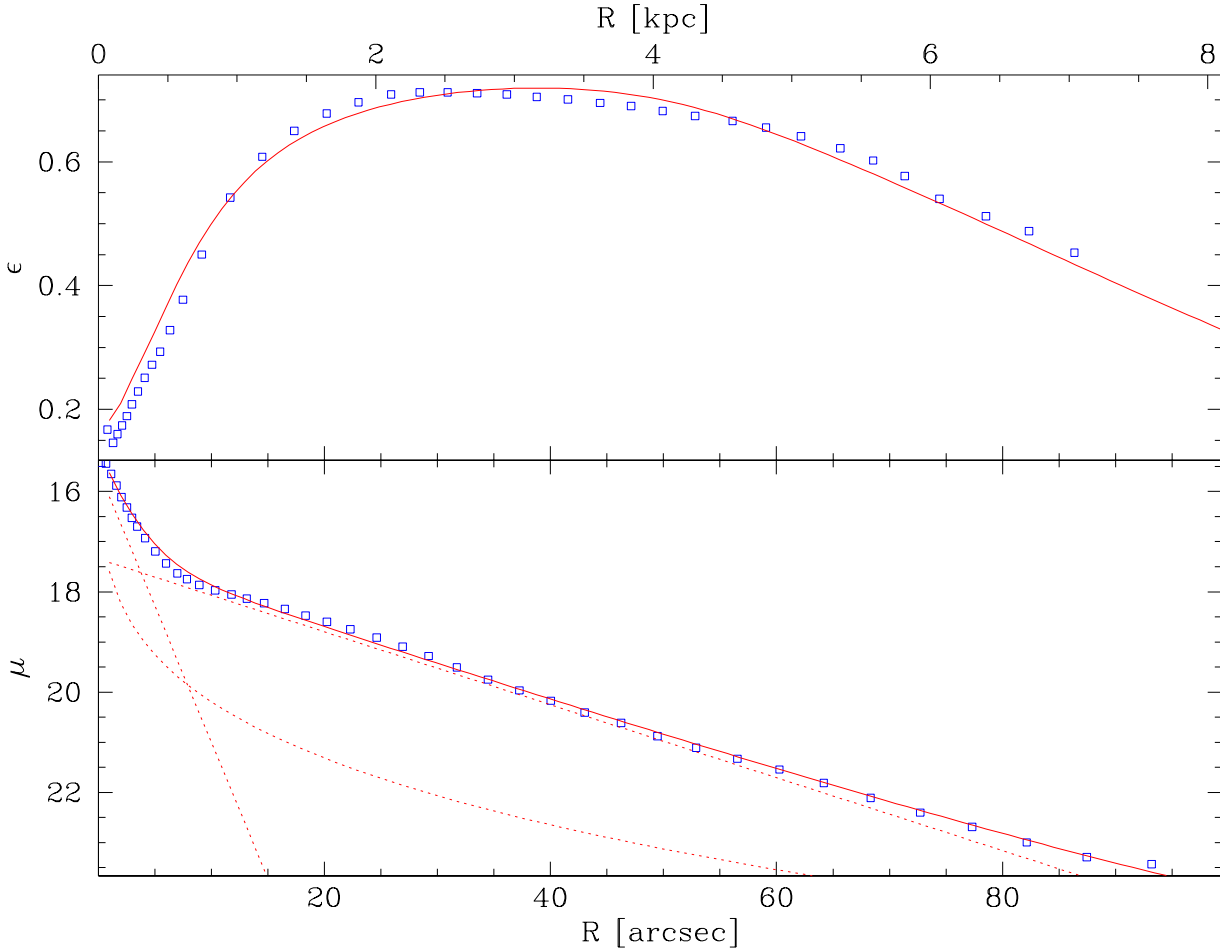


Figure 1. Photometric decomposition of NGC 4350. The parameters of the different components are shown in Table 2. Data are taken from Seifert and Scorza (1996). The dotted lines represent the separate contributions of the three different components to the global luminosity profile.

scale radius			axial ratio			Luminosity			i
r_b	r_d	r_h	$(b/a)_b$	$(b/a)_d$	$(b/a)_h$	L_b	L_d	L_h	
$2 \pm 0.^{\prime\prime}1$	$15 \pm 0.^{\prime\prime}2$	$40 \pm 6.^{\prime\prime}$	$1. \pm 0.03$	0.1 ± 0.01	0.95 ± 0.06	$24.5 \pm 4\%$	$26.5 \pm 1.5\%$	$49 \pm 5\%$	$85 \pm 5^{\circ}$

Table 2. Parameters of the decomposition shown in Fig. 1. The errors define the 1σ level in the parameter space on the basis of a reduced χ -square analysis.

indicated by the strong external decrease in the ellipticity profile (see Fig. 1).

In order to describe the photometry of this galaxy we have adopted a three-component model:

- (1) an almost edge-on exponential disc component;
- (2) a diffuse spheroidal component, with a deVaucouleur surface brightness profile, extending well beyond the disc itself, identified hereafter as “stellar halo”;
- (3) a second spheroidal component, very compact and with an *exponential* profile in the inner $2.^{\prime\prime}$ (see Fig. 1), which we identify as “bulge”.

The parameters derived by performing a best fit to the

photometric data are presented in Table 2, together with their statistical uncertainties.

The rapid increase in the ellipticity from very small values to a maximum of $\varepsilon \simeq 0.7$ at $r \approx 30.^{\prime\prime}$ (see Figure 1) and its slow decline in the outer parts can be explained if at least three components are used. The two “spheroidal” components may represent two physically different stellar systems, or, since the best-fit flattenings are very similar, a single, almost spherical component with a density profile not represented by the de Vaucouleur’s law (see discussion in the Section 5.2).

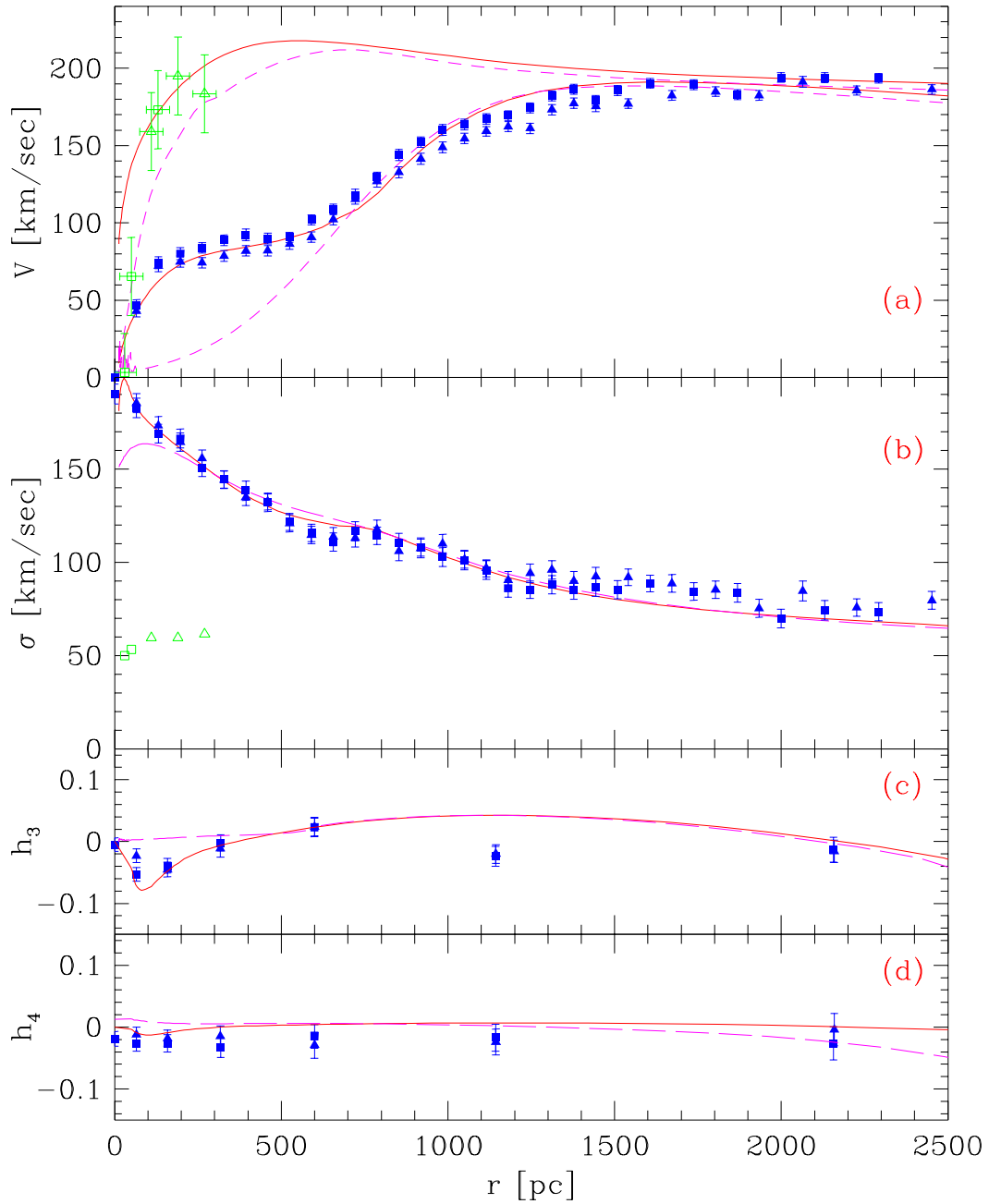


Figure 2. Data from Fisher (1997) for the major axis, compared with our best-fit models with (*solid line*) and without (*long-dashed line*) a central MDO. The squares and triangles represent data respectively from the approaching and the receding side. From the top: (a) stellar (*filled symbols*) and gas (*open symbols*) rotational velocities. The latter is also compared with the circular velocity inferred from the two models; (b) velocity dispersion profile; (c) h_3 radial profile; (d) h_4 radial profile. Data beyond 2.5 kpc are not shown because they were not included in the fit.

4.2 Kinematics

Fisher (1997) has published ground-based kinematics of 18 early-type galaxies, including NGC 4350. The data includes the stellar rotation curve, velocity dispersion profile and the line-of-sight velocity distribution described in terms of the

Gauss-Hermite expansion series terms h_3 and h_4 (Van Der Marel & Franx, 1993). Emission line spectroscopy reveals a disc of rapidly rotating gas within the inner 3'', which appears kinematically decoupled from the stellar component. In fact, while the gas is likely to follow circular orbits, the

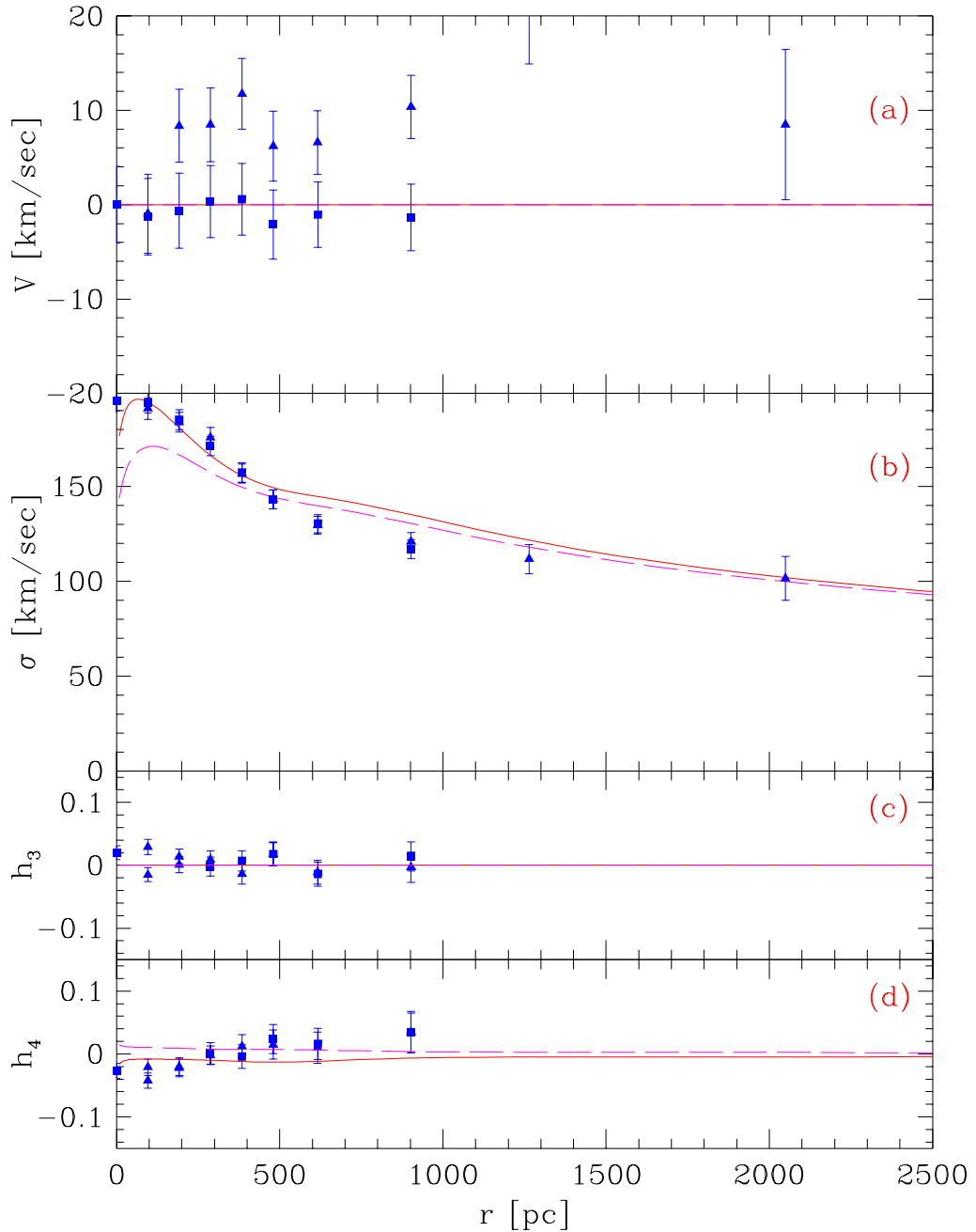


Figure 3. Data from Fisher (1997) for the minor axis, compared with our best-fit model with (solid line) and without (long-dashed line) a central massive dark object. The notation used for the symbols is the same as in Fig. 2.

stellar velocity is obtained by taking into account the asymmetric drift effect as

$$V_{\text{rot}}^2 = V_{\text{circ}}^2 - \Delta V_{\text{asymdrift}}^2, \quad (1)$$

where the $\Delta V_{\text{asymdrift}}^2$ (Binney & Tremaine, 1987) is essentially a function of the velocity dispersion and is only slightly dependent on the stellar distribution. The data are shown in Figs. 2-3.

Most parameters of the model have been fixed by fitting the photometry; the kinematic data are fitted by varying only the M/L ratios of the different stellar components and the value of the MDO mass.

A robust upper limit to the central mass of the MDO can be obtained by assuming that the gas follows a Keplerian rotation curve. After convolution with seeing and slit effects, we obtain $M_{\text{MDO}} \lesssim 1.5 \cdot 10^9 M_{\odot}$. However, since part of the gravitational force is due to the diffuse stellar component,

we allowed the value of the dark mass concentration to vary between zero and $M_{max} = 1.5 \cdot 10^9 M_\odot$. The value of the M/L ratios for the spheroidal components was allowed to vary from 1 to 10 times the corresponding value for the disc.

We integrated the Jeans equations as detailed in Pignatelli and Galletta (1999) to reproduce the kinematic data (see Figs. 2 – 3). The best-fit stellar M/L ratios spheroidal components and M_{MDO} are given in Table 3, together with their statistical uncertainties.

For the MDO model, the error bars were obtained by computing the reduced χ^2 for the whole grid of models, and rejecting the models with a reduced χ^2 greater than the 95% confidence level. For the non-MDO model, since the reduced χ^2 was very high for all of the models, we kept the models with a χ^2 greater than three times the minimum value.

From Figure 2 it is apparent that within 2.5 kpc the galaxy can be divided into 3 different regions:

(1) an inner region ($r < 120$ pc) which features a sharp increase in both the stellar and gas rotation curve. This implies that this region is dynamically dominated by the presence of the central dark massive object, which also determines the central cusp in the velocity dispersion profile.

(2) an intermediate region (120 pc $< r < 700$ pc) which is bulge-dominated. In this dynamically hot region the asymmetric drift effect dominates the stellar rotation curve, as shown by the large difference (~ 100 km/sec, i.e. a factor of more than 2) between the gas and the stellar velocities. The stellar rotational velocity reaches a plateau at about 50% of the circular velocity.

(3) an outer region ($r > 700$ pc) which is disc dominated. Here the stellar rotational velocity rises again, while the asymmetric drift effect plays a minor role. There is a probable flex point at $r \approx 900$ pc in the stellar velocity dispersion profile, as expected from the superposition of bulge and disc populations with different kinematical behaviour but similar masses.

Remarkably, these kinematic features match exactly those expected from photometric decomposition. This is not trivial: it implies that inside 2 kpc the light traces the mass, thus ruling out the possibility of a sizable presence of dark matter.

It is worthwhile to discuss in detail the differences between the best-fit MDO and non-MDO models in Fig. 2-3.

First, under the assumption of M/L ratios constant with radius for each component, the M/L values found in the two cases are similar (see Table 3) within the error bars given by the fit. This reflects the fact that in both cases the kinematics beyond $r = 500$ pc severely constrains all the parameters of the luminous matter in both cases.

The different panels of Fig. 2 show that the presence of the central massive object affects the different kinematical profiles up to different radii:

- The velocity dispersion profile is affected inside a “sphere of influence” of radius $r_{BH} = GM_{BH}/\sigma_0^2$. This is the radius at which the black hole is expected to increase the velocity dispersion by a factor $\sqrt{2}$. For the observed value of σ_0 and the inferred value of M_{BH} shown in Table 3, we expect r_{BH} to be about 70 pc, which is similar to what we see in Fig. 2b.
- While the velocity dispersion depends on the whole

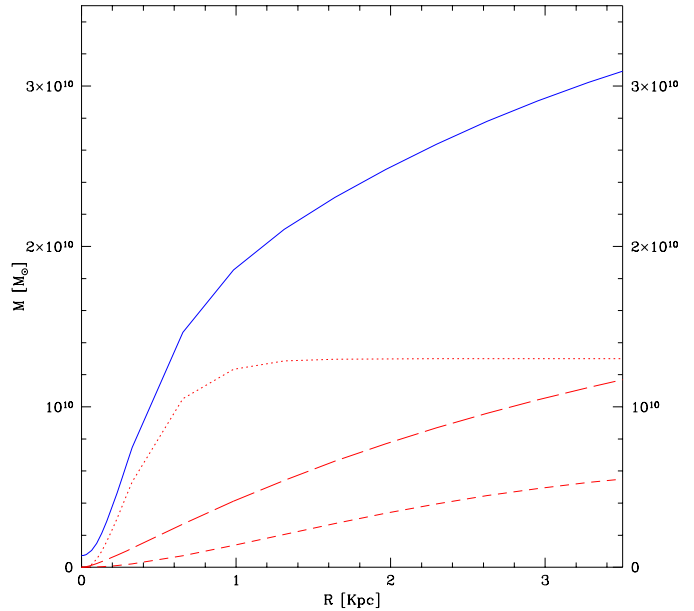


Figure 4. Luminous mass distribution of NGC 4350, according to Table 3. We plot the contribution of the inner exponential bulge (dotted line), the exponential disc (short-dashed line) and the outer deVaucouleur stellar halo (long-dashed line). The total mass is also shown as a solid line. Note that at $r = 0$ the mass is greater than zero because of the contribution from the MDO.

mass distribution, the circular velocity is only sensitive to the inner mass. The “radius of influence” in this case is the radius at which the stellar mass equals the MDO mass, and corresponds to about 200 pc, as can be seen in Fig. 4. At this radius the circular velocities of the MDO and non-MDO model differ by a factor $\sqrt{2}$, as shown in Fig. 2a. Beyond $r = 300$ pc part of these differences is due to the different stellar M/L ratios (see Table 3).

• The differences between the two models in the circular velocity are strongly amplified in the stellar rotation curve. For instance, at $r = 300$ pc, the MDO and non-MDO models have respective circular velocities of about 200 and 180 km/sec. Their asymmetric drift corrections $\Delta V_{asymdrift}$ account respectively for about 185 and 178 km/sec. If the rotational velocities are computed using Eq. (1), these small differences are magnified as shown in Fig. 2.

• Finally, the MDO affects the h_3 moment of the line-of-sight velocity distribution up to a similar radius ($r \approx 300$ pc). The h_3 signature, together with the gas rotation curve, are of great help in constraining the orbital anisotropies because they rule out strongly radial orbits in the inner part of the galaxy.

5 DISCUSSION

The photometric and kinematic data along both the major and minor axes have been explained through the superposition of different components: an inner MDO of mass $4.9 - 9.7 \cdot 10^8 M_\odot$, and three stellar components described in

	Model with MDO				MDO
	Bulge	Disc	Halo	MDO	
Mass	$(1.3 \pm 0.2) \cdot 10^{10} M_{\odot}$	$(7.1 \pm 0.7) \cdot 10^9 M_{\odot}$	$(2.7 \pm 0.3) \cdot 10^{10} M_{\odot}$	$(7.3 \pm 2.4) \cdot 10^8 M_{\odot}$	$(7.3 \pm 2.4) \cdot 10^8 M_{\odot}$
M/L	6.6 ± 0.9	3.3 ± 0.3	6.6 ± 0.7	—	
Model without MDO					
Mass	$(1.5 \pm 0.2) \cdot 10^{10} M_{\odot}$	$(6.6 \pm 0.7) \cdot 10^9 M_{\odot}$	$(2.8 \pm 0.3) \cdot 10^{10} M_{\odot}$	—	—
M/L	7.1 ± 1.0	3.1 ± 0.3	6.8 ± 0.6	—	—

Table 3. Masses of the different components for the best-fit models both with and without a central MDO. The error bars define the 95% confidence region in the parameter space, under the assumption that each component has a M/L ratio constant with radius. The mass profile derived for the model with a central MDO is shown in Fig. 4.

Table 3, with radial mass profiles $M(r)$ illustrated in Fig. 4. Each component is discussed separately hereafter.

5.1 The Massive Dark Object

The rotational velocities of both gas and stars are known to be much more efficient in constraining the mass of the central MDO than the velocity dispersion. Models without a central black hole fail to reproduce the shape of the inner rotation curve (see dot-dashed line in Fig. 2), unless unreasonable values of the bulge mass-to-light ratio are assumed which, however, would imply velocity dispersions much larger than those observed. In the inner kpc, the reduced chi-square is $\chi \sim 1.77$ for the best-fit model with MDO, and $\chi \sim 100$ for the model without MDO.

On the other hand, the errors given in Table 3 are just statistical errors. We must consider also possible systematic errors related to the assumptions used in the model.

The main concern is related to different hypotheses on the phase-space distribution function of the stellar component. So far, the model we presented is axisymmetric, with an isotropic velocity distribution. Such a model is associated with a distribution function which only depends on the two classical integrals of motion, i.e. energy and vertical angular momentum: $f = f(E, L_z)$. However, strong radial anisotropy in the centre of the galaxy results in a high velocity dispersions, mimicking the presence of a MDO (Gebhardt *et al.*, 2000b).

For this specific galaxy, significant anisotropies in the velocity distribution would certainly raise the central velocity dispersion of the non-MDO model up to the observed value, but: (i) the gas rotational velocity, which is unaffected by the isotropic hypothesis, would be too low with respect to the observations; (ii) the stellar rotational velocity would decrease, moving away from the observations; (iii) The radial orbits in the central bin would increase the h_4 parameter, in contrast with that suggested by the data. Thus, in this galaxy the hypothesis of radial orbits can not reduce the estimated MDO mass.

In principle, we cannot exclude the possibility that, inside the innermost observed kinematical point, the M/L ratio of the stellar component is rising sharply enough to mimic the presence of a massive dark object. However, the innermost observed kinematical point is at $R_{\text{inner}} \sim 0''.6 = 66$ pc, and the data requires a dynamical mass inside this point of $1.1 \cdot 10^9 M_{\odot}$, which, compared with the observed pho-

tometry, implies an $M/L \approx 28$ in this region, much higher than the value $M/L \approx 11.5$ found by Loyer *et al.* (1998). Such a high mass-to-light ratio seems unlikely for any given choice of stellar population (Worthey, 1994). Adopting an extreme $M/L \approx 12$ for the innermost region would only reduce the best-fit M_{MDO} to $5 \cdot 10^8 M_{\odot}$, and the lower limit to $2.5 \cdot 10^8 M_{\odot}$.

In addition, we have not forced the whole galaxy to have the same stellar mass-to-light ratio. Instead, we allowed different M/L ratios for different components, although the best model fit suggests similar values for the bulge and stellar halo. This seems a reasonable hypothesis because it links every dynamical component to a given star formation history. The M/L ratio of our global stellar component increases with decreasing radius.

Finally, the hypothesis of constant flattening for each photometric component is also a possible source of systematic errors. Because of this assumption, we obtained a photometric decomposition with small statistical errors (see Table 2), despite the large seeing (about $2''.5$) of the ground-based observations. If we relax this hypothesis, then it is possible that the stellar component becomes flatter inside the seeing radius, contributing to the rotation shown in Fig. 2 and reducing the need for a central MDO.

We can not reproduce this kind of behaviour in a self-consistent way with our model. We can, however, give an estimate of the systematic errors involved, evaluating a set of models with different ellipticities for the bulge component, and trying to reproduce the stellar V and σ profile only in the inner $2''$. In order to fit the inner rotation curve without MDO, all the mass inside $2''$ must flatten to $\epsilon \gtrsim 0.3$. On the other hand with $\epsilon = 0.3$, the central velocity dispersion falls below the predictions for the no MDO case with $\epsilon = 0$ and does not match the observations (cfr. Fig. 2). Under the assumptions of $M/L = 12$ for the bulge and $\epsilon \simeq 0.2$ within $2.5''$, both the inner rotation velocity and dispersion velocity can be fitted within the error bars, if a central dark object with $M_{\text{MDO}} \approx 1.5 \cdot 10^8$ is present.

Taking into account all the above listed source of uncertainties, the dark object mass falls in the range $1.5 \lesssim M_{\text{MDO}} \lesssim 9.7 \cdot 10^8$, implying $-2 \lesssim \log(M_{\text{MDO}}/M_{\text{bulge}}) \lesssim -1.1$. This wide range is substantially due to the poor resolution of the available data.

We can now locate NGC 4350 in the $\sigma_e - M_{\text{MDO}}$ plane. Following the same prescription as in Gebhardt *et al.* (2000a), we computed for NGC 4350 a luminosity-weighted

$\sigma_e = 180$ km/s inside R_e . The relationship found by Gebhardt et al. (2000a) would predict for this value $6.5 \times 10^7 \leq M_{MDO} \leq 9.7 \times 10^7$. Although our best estimate is a factor of 10 larger than the value expected on the basis of $\sigma_e - M_{MDO}$ relationship, nevertheless our lower limit is quite close to the expected range. In this context it is worth noticing that NGC 4350 was selected for our analysis on the basis of the high velocity rotation of its nuclear gas.

It is interesting to compare our results with those given in Loyer et al. (1998). Adopting a single M/L ratio of 7 for the whole stellar population, they found that the inner kinematics required a central point mass of $M = 8 \cdot 10^8 M_\odot$, a result that agrees very well with our value of $M_{MDO} = 7.3 \cdot 10^8 M_\odot$, despite the difference in the methods adopted. However, the evidence for a MDO was marginal. The difference between our results and those of Loyer et al. (1998) is due to the different dataset adopted: in particular, the fact that we included both the gas and star kinematics, and especially the h_3 and h_4 profiles, dramatically increases the constraints we can put on the M_{MDO} . This is especially true in the inner 5'', where the shape of the line-of-sight velocity distribution is strongly non-gaussian (see Fig. 2), corroborating the conclusion that the search for an MDO is much more effective if the analysis of the higher orders of the line-of-sight velocity distribution is included (Cretton & Van Den Bosch, 1999).

5.2 The stellar component

The photometry of this galaxy can not be described by a simple superposition of a deVaucouleur spheroid and an exponential disc. The addition of a third spheroidal component is required. However, the fact that the mass-to-light ratios that reproduce the kinematical data for the two spheroidal components are similar suggests that there is a single, almost spherical stellar population; its brightness profile follows the deVaucouleurs law only up to the inner ≈ 600 pc, and then starts to diverge towards a much steeper inner surface brightness profile. This behaviour agrees with recent HST high resolution photometric data (Lauer *et al.*, 1995) showing that many ellipticals and bulges do have inner cusps steeper than expected from the $r^{1/4}$ law, with a luminosity density profile $I(r) \sim r^{-\gamma}$, with $\gamma \sim 1$ for 5 pc $< r < 1$ kpc. In addition, Faber *et al.* (1997) have shown that this behaviour is more evident in rapidly rotating, disk bulges such as the one in NGC 4350.

A possible relation between the presence of a central BH and the inner surface brightness profile has been extensively investigated by several authors (Young, 1980; Van Der Marel, 1999) in the framework of adiabatic black hole growth. The effect on the photometry, however, can only be seen in the "sphere of influence" of radius $r_{BH} = GM_{BH}/\sigma_0^2$, that we showed to be about 70 pc, which is less than 1'' at Virgo distance. Our poor angular resolution did not allow us to check for this effect.

It is noteworthy that the mass-to-light ratio obtained for the spheroidal component ($(M/L)_{sph} = 6.6 \pm 0.7$) is in good agreement with the relation by van der Marel (1991), which yields $(M/L)_{sph} = 4.8 \pm 1.5$ for a galaxy of this luminosity. At the same time, the value we found for the disc ($(M/L)_D = 3.3 \pm 0.3$) is in agreement with Salucci & Persic (1999), that give $(M/L)_D \approx 2.5 \pm 0.5$ at this luminosity.

We expect this difference in the M/L ratio of the two components to be visible in the colour distribution of the galaxy. There is indeed evidence for a colour gradient, going from $(B - V) = 1.1$ in the inner, bulge-dominated region, to a $(B - V) \approx 0.84$ in the intermediate region (Prugniel & Heraudeau, 1998), which qualitatively agrees with our results.

5.3 The dark matter halo

In the previous sections, we purposely limited ourselves to the inner regions of the galaxy ($r \leq 2R_d$), since here the diffuse dark matter component is clearly not required by the data.

A complete and detailed investigation of the dark matter distribution in NGC 4350 is beyond the scope of this paper. Nevertheless, under the hypotheses described above, it is possible to derive a preliminary estimate on the mass and distribution of dark matter needed to explain the kinematical data in the outer regions.

The observed velocity (Fisher, 1997) is nearly circular and almost flat in the range $1.8 \leq r \leq 3.5$ kpc. It can be represented by a linear law $V(R) = (175 \pm 5) + (3.6 \pm 1.2)r$, where r is expressed in kpc and V in km/sec. With the stellar distribution we derived in Table 3, this implies that within the last observed kinematical point $R_{last} \approx 3.5$ kpc the dark matter amounts to $M_{DM} = 1.2 \cdot 10^{10} M_\odot$, which is 30% of the total mass inside this point. The DM density should equal that of the luminous matter at $R \approx 3$ kpc, so that, as observed in spiral galaxies (Salucci & Persic, 1999), in the inner regions the light traces the dynamic mass.

6 CONCLUSIONS

From the photometric and kinematic data available in the literature, we inferred the mass distribution for the S0 galaxy NGC 4350. The data used to constrain the model include: R-band photometry, rotational velocity of gas and stars and velocity dispersion profiles along both the major and minor axis, and the h_3 and h_4 profiles, for a total number of 280 data points. Our results can be summarized as follow:

- An MDO of $M \approx 1.5 - 9.7 \cdot 10^8 M_\odot$ is located at the centre of the galaxy. A lower value for the central mass is possible if we allow for a very sharp increase of the anisotropy in the velocity distribution. However, this could be obtained only by neglecting the information content in the gas kinematics and the h_3 and h_4 parameters profiles.

- This galaxy falls in the upper envelope of the $M_{bulge} - M_{BH}$ or $\sigma_e - M_{BH}$ relations known so far. This is expected, given that it has been selected for the very fast rotation of its nuclear disc.

- The estimated stellar M/L ratios (~ 6.6 for the spheroid and ~ 3.3 for the disc) are in agreement with the average values usually found for these components. In order to explain the mass concentration in the centre of NGC 4350, the stellar M/L ratio has to increase in the innermost 60 pc from the average value of 6.6 to ~ 28 . Such a high value is, however, ruled out by the comparison between the observed colours and synthetic stellar population models.

- Within the hypothesis of the model, the kinematical data between 2.5 and 3.5 kpc imply that the DM density equalizes that of the luminous matter at $R \approx 3$ kpc, and that the dark matter mass is 30% of the total within $r = 3.5$ kpc.

Acknowledgements. We thank the referee, Dr. K. Gebhardt, for helpful comments and suggestions that greatly improved the quality of the paper.

REFERENCES

Binney, J. and Tremaine, 1987. *Galactic Dynamics*. Princeton University Press.

Cretton, N. and Van Den Bosch, F. C., 1999, ApJ, 514, 704.

Emsellem, E., Dejonghe, H., and Bacon, R., 1999, MNRAS, 303, 495.

Faber, S. M., Tremaine, S., Ajhar, E. A., Byun, Y. I., Dressler, A., Gebhardt, K., Grillmair, C., Kormendy, J., Lauer, T. R., and Richstone, D., 1997, AJ, 114, 1771.

Ferrarese, L. and Merritt, D., 2000, preprint, astro-ph/0006053.

Fisher, D., 1997, AJ, 113, 950.

Ford, H. C., Tsvetanov, Z., Ferrarese, L., Dressel, L., and Jaffe, W., 1999, in: Galaxy Interactions at High and Low redshift, Proceedings of the IAU conference held in Kyoto, Japan, August 26-30, 1997. eds. D.B. Sanders and J. Barnes, Kluwer.

Gebhardt, K., Bender, R., Bower, G., Dressler, A., Faber, S. M., Filippenko, A., Green, R., Grillmair, C., Ho, L., Kormendy, J., Lauer, T. R., Magorrian, J., Pinkney, J., Richstone, D., and Tremaine, S., 2000, preprint, astro-ph/0006289.

Gebhardt, K., Richstone, D., Kormendy, J., Lauer, T. R., Ajhar, E. A., Bender, R., Dressler, A., Faber, S. M., Grillmair, C., Magorrian, J., and Tremaine, S., 2000, AJ, 119, 1157.

Ho, L., 1999, in: Observational Evidence for the Black Holes in the Universe, p. 157.

Kormendy, J. and Richstone, D., 1995, ARA&A, 33, 581.

Kormendy, J., Bender, R., Ajhar, E. A., Dressler, A., Faber, S. M., Gebhardt, K., Grillmair, C., Lauer, T. R., Richstone, D., and Tremaine, S., 1996, ApJ, 473, L91.

Lauer, T. R., Ajhar, E. A., Byun, Y. I., Dressler, A., Faber, S. M., Grillmair, C., Kormendy, J., Richstone, D., and Tremaine, S., 1995, AJ, 110, 2622.

Loyer, E., Simien, F., Michard, R., and Prugniel, P., 1998, A&A, 334, 805.

Magorrian, J., Tremaine, S., Richstone, D., Bender, R., Bower, G., Dressler, A., Faber, S. M., Gebhardt, K., Green, R., Grillmair, C., Kormendy, J., and Lauer, T., 1998, AJ, 115, 2285.

Pignatelli, E. and Galletta, G., 1999, A&A, 349, 369.

Prugniel, P. and Heraudeau, P., 1998, A&AS, 128, 299.

Salucci, P. and Persic, M., 1999, MNRAS, 309, 923.

Salucci, P., Szuszkiewicz, E., Monaco, P., and Danese, L., 1999, MNRAS, 307, 637.

Salucci, P., Ratnam, C., Monaco, P., and Danese, L., 2000, MNRAS, in press.

Seifert, W. and Scorza, C., 1996, A&A, 310, 75.

Tsvetanov, Z. I., Pei, Y. C., Ford, H. C., Kriss, G. A., and Harms, R. J., 1998, in: American Astronomical Society Meeting, Vol. 193, p. 119.01.

Tully, R. B., 1988. *Nearby galaxies catalog*. Cambridge and New York, Cambridge University Press, 1988, 221 p.

Van Der Marel, R. P., 1991, MNRAS, 253, 710.

Van Der Marel, R. P., 1999, AJ, 117, 744.

Van Der Marel, R. P. and Franx, M., 1993, ApJ, 407, 525.

Worley, G., 1994, ApJS, 95, 107.

Young, P., 1980, ApJ, 242, 1232.